Deep Learning a Quadrotor Dynamic Model for Multi-Step Prediction

Nima Mohajerin, Melissa Mozifian and Steven Waslander[1]

***Abstract*— In this work, we develop and assess models for a real quadrotor in a Multi-Step prediction problem, that is, predicting the system state over many future steps using only the input. We propose a hybrid model with two configurations by combining deep recurrent neural networks with a quadrotor motion model. The proposed models take only motor speeds as input and predict the system state over a prediction length as long as 2 seconds. Network state initialization is performed and the effect of state initialization is shown in our results. Our experiments, evaluated on our collected real quadrotor dataset, show that the proposed models outperform the rigid body dynamics model, commonly used in quadrotor control, as well as a black-box model in both single-step and multi-step prediction scenarios.**

I. Introduction

In this paper, we propose models for a real quadrotor using first principles and deep learning methods for the Multi-Step (MS) prediction task. Our proposed models can accurately predict the quadrotor behaviour over many steps into the future, given only the motor speeds as input. In the MS prediction, the model is used in a closed loop fashion; an input *sequence* (or *trajectory*) is given to the model along with an initial state and the model recursively predicts the system state over a prediction horizon. This causes the unmodeled dynamics and accumulated noise error to drastically deteriorate the prediction accuracy. Despite such challenges, MS prediction has proven useful in control and simulation settings [1], [2].

Traditionally, a model is developed based on the first principles and then the parameters of the model, such as mass, are identified [3], [4]. Such model is called a *white-box* (WB) or a *first principle* model. Identifying the parameters of a white-box model may require an expensive procedure. For instance, measuring the blade drag coefficient of a quadrotor needs a wind tunnel. Additionally, many properties of the system may be too difficult to formulate. For instance, modeling the aerodynamic effects on quadrotors is difficult. Due to their light weight, quadrotors are very susceptible to aerodynamic effects. Nevertheless, a quadrotor always obeys the rigid-body dynamics. In this work, we develop a novel hybrid model for a quadrotor by combining the rigid-body dynamics with Recurrent Neural Networks (RNNs) in two configurations. Our proposed model learns the quadrotor model parameters and the network weights using the observations from the real system.

[1]Nima Mohajerin, Melissa Mozifian and Steven Waslander are with Faculty of Mechanical and Mechatronics Engineering, University of Waterloo, Waterloo, ON, Canada. (nima.mohajerin, melissa.mozifian, stevenw)@uwaterloo.ca

Modeling the dynamics of a quadrotor has been studied extensively in [5], [6], [7], [8], [9], [10], [11]. First principle models of quadrotors have also been used in control [12], [13], [14]. However, they are only valid around hover and do not include the aerodynamic effects such as the vortex effect. Additionally, these models are used in a Single-Step (SS) prediction scenario, where the prediction is required over one step into the future, given the current system state and the input. Using these models in an MS prediction fashion, the predicted states rapidly diverge as we will demonstrate in this work.

Few existing methods use deep learning techniques to model aerial vehicles. Abbeel et al. employed Feed Forward Neural Networks (FFNNs) with Rectified Linear Units (ReLUs) to model a real helicopter in an SS fashion [15]. A similar approach was adopted in modeling a quadrotor [16], for SS prediction and control. Recently black-box (BB) models (models that are fully learned from data) have been developed using RNNs for quadrotors [17], [18], [19], [20]. In [17], an Echo-State RNN is used to model a quadrotor from experimental data. Although not explicitly stated, their results show an SS prediction scenario. In [20], a deep RNN is used to model the dynamic of the altitude of a real quadrotor. It is also shown that the model significantly outperforms the first principle model in MS prediction scenarios. In this work, a similar approach to [20] is adopted to generate a full BB model of a quadrotor and the results are compared with our proposed hybrid approach.

In [21] a hybrid of neuro-fuzzy and a parameteric structured model is used to model a quadrotor for SS prediction. Our approach is similar, however, we use deep Long-Short-Term-Memory (LSTM) networks [22] in conjunction with a motion model of a quadrotor derived from laws of rigid-body dynamics. We evaluate our approach by comparing against a full RNN based BB model and an instance of first principle model in MS prediction scenarios. Experiments show that our hybrid model significantly outperforms both models evaluated on a real quadrotor dataset. Our hybrid model predict the vehicle velocity and body rates over almost 2 seconds with the errors less than 10 cm/sec and 7 deg/sec. In 40 steps prediction (0.4s flight time), the hybrid-model error is less than 4 cm/sec and 1.5 deg/sec.

This paper is orginized as follows. The MS prediction problem is formulated in Section II. Section III describes the quadrotor models under consideration. Section IV describes the hardware configuration and the collected dataset. Section V illustrates the results and comparisons. Finally, Section VI concludes the paper.

II. MS Prediction Problem Formulation

Consider a dynamic system $\mathcal{S}_n^m$ with m input and n output dimensions in discrete time domain. The system input and output at a time instance, k, is denoted by $\mathbf{u}(k) \in \mathbb{R}^m$ and $\mathbf{y}(k) \in \mathbb{R}^n$, respectively. It is assumed that both input and output are measurable at all ks. Consider an input sequence of length T starting at a time instance k_0+1, $\mathbf{U}(k_0+1, T) \in \mathbb{R}^m \times \mathbb{R}^T$,

$$\mathbf{U}(k_0+1, T) = \begin{bmatrix}\mathbf{u}(k_0+1) & \mathbf{u}(k_0+2) & \dots & \mathbf{u}(k_0+T)\end{bmatrix}. \tag{1}$$

The system response to this input is an output sequence denoted by $\mathbf{Y}(k_0+1, T) \in \mathbb{R}^n \times \mathbb{R}^T$,

$$\mathbf{Y}(k_0+1, T) = \begin{bmatrix}\mathbf{y}(k_0+1) & \mathbf{y}(k_0+2) & \dots & \mathbf{y}(k_0+T)\end{bmatrix}.$$

Given an input sequence $\mathbf{U}(k_0+1, T)$, the multi-step (MS) prediction problem seeks an accurate estimate of the system output over the same time-horizon, $\tilde{\mathbf{Y}}(k_0+1, T) \in \mathbb{R}^n \times \mathbb{R}^T$,

$$\tilde{\mathbf{Y}}(k_0+1, T) = \begin{bmatrix}\tilde{\mathbf{y}}(k_0+1) & \tilde{\mathbf{y}}(k_0+2) & \dots & \tilde{\mathbf{y}}(k_0+T)\end{bmatrix}, \tag{2}$$

which minimizes a measure of distance between the actual and predicted outputs. Typically, a Sum-of-Squares Error measure (SSE) is chosen,

$$L = \frac{1}{T}\sum_{k=k_0+1}^{k_0+T} \mathbf{e}(k)^\top \mathbf{e}(k), \tag{3}$$

$$\mathbf{e}(k) = \mathbf{y}(k) - \tilde{\mathbf{y}}(k). \tag{4}$$

In the above equations, $\mathbf{e}(k)$ is the prediction error at the kth prediction step.

III. Models for a Quadrotor

A quadrotor is a rotorcraft aerial vehicle which generates its lift by two pairs of identical fixed pitched propellers. In the commonly used quadrotors, each pair is mounted at the two ends of an arm and the two arms are attached at the center. The propellers of each pair rotate in the same direction which opposes the direction of rotation of the other pair.

The models described in this section are implemented in discrete time domain. In an MS prediction scenario, they receive a sequence of motor speeds over a prediction length, as in (1), and generate a sequence of body rates and velocities, as in (2).

A. First Principle Model

We adopt the model described in [14]. For convenience we treat the variables in the continuous time domain in this section only. The quadrotor state vector is formed as follows,

$$\begin{aligned}\mathbf{x}^\top &= [x_1\ x_2\ x_3\ x_4\ x_5\ x_6\ x_7\ x_8\ x_9\ x_{10}\ x_{11}\ x_{12}] \\ &= [\boldsymbol{\eta}^\top\ \boldsymbol{\omega}^\top\ \boldsymbol{\xi}^\top\ \dot{\boldsymbol{\xi}}^\top] \\ &= [\phi\ \theta\ \psi\ p\ q\ r\ x_I\ y_I\ z_I\ \dot{x}_I\ \dot{y}_I\ \dot{z}_I],\end{aligned} \tag{5}$$

where ϕ, θ and ψ are the Euler angles, i.e. roll, pitch and yaw, respectively (Figure 1). Body rates are denoted by $\boldsymbol{\omega}^\top = [p, q, r]$ and position by $\boldsymbol{\xi}^\top = [x_I, y_I, z_I]$. The equations governing the dynamic of a quadrotor are,

$$\begin{aligned}\dot{x}_1 &= x_4 + x_5 S_1 T_2 + x_6 C_1 T_2 \\ \dot{x}_2 &= x_5 C_1 - x_6 S_1 \\ \dot{x}_3 &= \sec(x_2)(x_5 S_1 + x_6 C_1) \\ \dot{x}_4 &= -((I_z - I_y)/I_x) x_5 x_6 - (k_r x_4 / I_x) + (1/I_x)\tau_p \\ \dot{x}_5 &= -((I_x - I_z)/I_y) x_4 x_6 - (k_r x_5 / I_y) + (1/I_y)\tau_q \\ \dot{x}_6 &= -((I_y - I_x)/I_z) x_4 x_5 - (k_r x_6 / I_z) + (1/I_z)\tau_r \\ \dot{x}_7 &= x_{10}, \quad \dot{x}_8 = x_{11}, \quad \dot{x}_9 = x_{12} \\ \dot{x}_{10} &= (-k_t x_{10}/m) + (1/m)(C_1 S_2 C_3 + S_1 S_3)\tau_f \\ \dot{x}_{11} &= (-k_t x_{11}/m) + (1/m)(C_1 S_2 S_3 - S_1 C_3)\tau_f \\ \dot{x}_{12} &= (-k_t x_{12}/m) + (1/m)(C_1 C_2)\tau_f - g,\end{aligned} \tag{6}$$

where, I_x, I_y, I_z represent inertia, m represents mass of the quadrotor, k_t and k_r represent the translational and rotational drag coefficients and are assumed to be constant in all directions for simplicity. Also, $T_i = \tan(x_i)$, $S_i = \sin(x_i)$ and $C_i = \cos x_i$. The control inputs are represented by τ_p, τ_q, τ_r, which are the moments about the three axes, and τ_f, which is the total thrust acting on the vehicle. The acceleration due to gravity is represented by g.

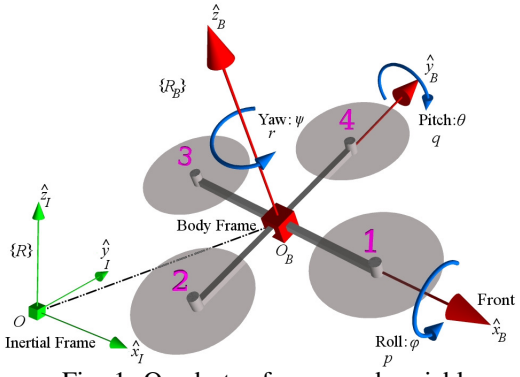

Fig. 1: Quadrotor frames and variables.

In [14], the control inputs are generated by the following mapping from the motor speed,

$$\begin{bmatrix}\tau_f \\ \tau_p \\ \tau_q \\ \tau_r\end{bmatrix} = \begin{bmatrix}1 & 1 & 1 & 1 \\ 0 & -l & 0 & l \\ -l & 0 & l & 0 \\ -d & d & -d & d\end{bmatrix} \begin{bmatrix}f_1 \\ f_2 \\ f_3 \\ f_4\end{bmatrix}, \tag{7}$$

given the directions and motor numbering depicted in Figure 1. In equation (7) l is the distance from the center of mass to the rotors, d is the ratio between the drag and the thrust coefficients of the blade, and f_i for $i = \{1, 2, 3, 4\}$ are the forces generated by the four rotors of the quadrotor which are related to the rotor speeds, u_i, by the following equation,

$$f_i = \frac{b_i + u_i^2}{k_i} \tag{8}$$

where b_i and k_i are identified for each motor. The mapping depicted by equation (7) is only used for the WB model in this work.

B. Full Black-box Model

Using RNNs, it is possible to learn a dynamic model of a quadrotor from observations [18], [19]. In an MS prediction scenario, the input to the RNN is a sequence of the motor speeds and the RNN generates the quadrotor states. Therefore, each training instance is a tuple of two equal-length time-series, an input, which is the motor speeds, and an output, which encompasses the quadrotor states. As described in [20], an RNN should be properly initialized to accurately predict the system states. The authors in [20] addressed the state initialization problem and demonstrated that the proposed architecture for modeling the altitude of a real quadrotor outperforms the first principle model described above. This work applies the same initialization method to LSTM networks.

The state initialization procedure proposed in [20] splits the input and output sequences of each training instance into two segments. The first segment of the input and output are fed to an FFNN (the initializer network) which generates the initial state values for the RNN (the predictor). The second segment is used for prediction; the input segment is fed to the RNN and it is trained to learn the output segment. In this work, we adopt the same method to initialize the hidden and cell states of LSTM networks to learn a full BB model. LSTM networks consist of layers of LSTM cells. The gated architecture of LSTMs helps to retain relevant information across time. There are many versions of LSTMs [23]. In this work, we use the version described in [24] which are equipped with *peephole* connections.

In this work, we use networks with multiple layers of LSTM cells connected in a serial fashion. The networks may also benefit from input and output buffers or *Tapped Delay Lines* (TDLs) [25]. The following notation is used to state a network architecture, network-type : number of layers $\times$ number of cells. For instance, a network with 5 layers, each having 200 cells, and input/output TDLs is depicted as LSTM TDL:5$\times$200.

C. Hybrid Model

We propose a hybrid model which comprises three modules; an Input Modeler (IM), a Motion Model (MM) and an Output Modeler (OM). Using rigid body dynamics, the MM module implements the motion model of a quadrotor i.e. the descritized version of the equations (6). The IM module provides the input to the MM module, $\tilde{\boldsymbol{\tau}}$, which has four elements that are plugged into the equations (6) as τ_p, τ_q, τ_r and τ_f. The OM module compensates for the deviation of the MM module output from the desired values. The IM and OM are deep RNNs with LSTM cells initialized by the initialization scheme discussed in [20]. Depending on the three module connectivities, two architectures are proposed:

1) ***Hybrid-Serial Configuration****:* This configuration is illustrated in Figure 2. The blue connections are the feedback and the black are the feedforward connections. The model output is directly provided by the OM module. The gains $\mathbf{w}_\omega$ and $\mathbf{w}_{\dot{\xi}}$ are the normalization factors. Note that the output of the MM does not receive any penalty directly; the error goes through the OM module and reaches the MM and IM modules. The hybrid-serial configuration assumes no prior relation between part of the system that is modelled by the MM module and the unmodelled part, which is learned from the observations during training.

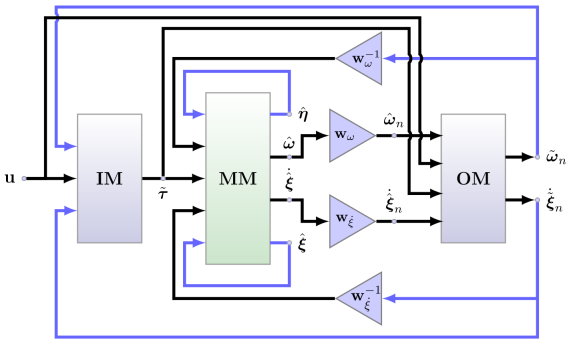

Fig. 2: Proposed hybrid-serial model.

2) ***Hybrid-Parallel Configuration****:* A possible scenario in the hybrid-serial configuration is that the RNNs takes control and attenuate the influence of MM. Since the RNNs have many degrees of freedom, this case is not necessarily inevitable. One possible solution is to directly incorporate the output of the MM module in the model output. This is depicted in Figure 3. The underlying assumption in this configuration is that the modeling error of the MM module can be represented by an additive term, i.e. the output of the OM module. In this configuration, the OM module acts as a compensator which predicts and eliminates error in the MM module.

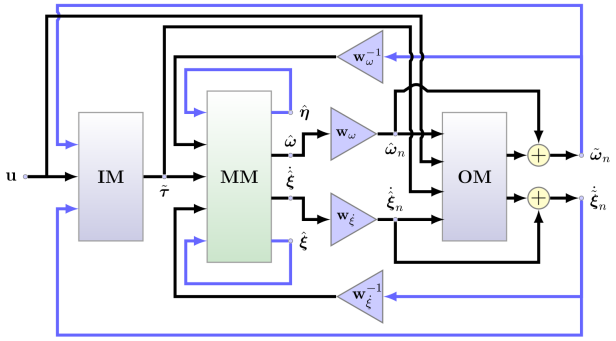

Fig. 3: Proposed hybrid-parallel model.

IV. The Quadrotor Dataset

The modeling approaches considered in this work is applied to the AscTec Pelican[1]. It is a light weight quadrotor equipped with a real-time autopilot board coupled with an onboard computer(AscTec Mastermind). The onboard computer communicates with the autopilot board via a UART connection and runs a ROS node[2] to collect the motor speeds and Inertial Measurement Unit (IMU) readings. The vehicle is operated in an indoor environment by an expert pilot using

[1] http://www.asctec.de/en/uav-uas-drones-rpas-roav/asctec-pelican/

[2] http://wiki.ros.org/asctec_mav_framework

a Futaba T7C remote control. The dataset we have collected is publicly available.[3]

The vehicle position and inertial orientation are measured at 100 Hz using a Vicon motion capture system[4], equipped with 16 Vantage cameras looking at the IR reflective markers mounted on the vehicle. These measurements are then sent to the Vicon server through a LAN communication. To avoid any wireless latency and/or packet drops, the measurements are logged on the Vicon server computer using the Vicon Tracker software version 3.3 and then synchronized with the autopilot measurements offline. The Vicon system is calibrated before each data collection session to account for changes in environmental variables, such as room temperature, camera body, temperature, etc.

The quantities included in the quadrotor dataset are

- motor speed, $\mathbf{u}(k) = [u_1(k), u_2(k), u_3(k), u_4(k)]$,
- velocity vector, $\boldsymbol{\xi}(k) = [\dot{x}_I(k), \dot{y}_I(k), \dot{z}_I(k)]$,
- body rates, $\dot{\boldsymbol{\omega}}(k) = [p(k), q(k), r(k)]$.

The dataset consists of various flight regimes; hover, close to ground, light, moderate and aggressive manoeuvres in all directions. The dataset total flight time is approximately 3 hours and 50 minutes. The total number of samples per each element of each quantity is 1388410. The data is split into 60%, used for training and 40% for generalization testing.

V. Results

The quadrotor is modelled as a Multi-Input-Multi-Output (MIMO) system, which receives the motor speeds trajectory and predicts the vehicle body rates and velocity (in inertial frame). The BB and hybrid models are implemented using Google's Tensorflow library [26] in Python. The network training and inference was performed using a GeForce Titan Xp GPU. For evaluation, the prediction error and its distribution are studied. The prediction error is defined at each prediction step as in equation (4). We take the mean of the absolute value of the velocity and the body rate errors on the three axes and compare the distribution over the prediction steps,

$$\begin{aligned} \bar{e}_{\dot{\xi}}(k) &= \tfrac{1}{3}\big(|e_{\dot{x}_I}(k)| + |e_{\dot{y}_I}(k)| + |e_{\dot{z}_I}(k)|\big), \\ \bar{e}_{\omega}(k) &= \tfrac{1}{3}\big(|e_p(k)| + |e_q(k)| + |e_r(k)|\big), \end{aligned} \tag{9}$$

where $\bar{e}_{\dot{\xi}}(k)$ is in meters per second (m/s) and $\bar{e}_{\omega}(k)$ is in degrees per second (deg/sec).

A. White-box parameter identification

The drag coefficients and the motor parameters for the first principle model are identified using a Least-Squares (LS) method. Since the first principle model is valid around hover, LS is applied to the near hover flight regimes. The inertias (I_x, I_y and I_z), mass m and the identified parameters are listed in Table I. Note that the flight volume is not large enough to capture the drag coefficient, k_r. As a result LS identifies this parameter close to zero.

[3] https://github.com/wavelab/pelican_dataset

[4] https://www.vicon.com/products/camera-systems

k_r	k_t	b_1	k_1	b_2
0.0099	2.35×10^{-14}	0.062	7.63×10^{6}	0.082
k_2	b_3	k_3	b_4	k_4
1.21×10^{7}	0.0016	4.67×10^{6}	2.28×10^{-4}	4.69×10^{6}

$I_x(kg.m^2)$	$I_y(kg.m^2)$	$I_z(kg.m^2)$	$m(kg)$	$l(m)$
0.002	0.002	0.001	1.6	0.211

TABLE I: Quadrotor WB parameters.

For validating the model, however, the entire dataset is used. The model is employed in two scenarios; an SS prediction and an MS prediction over 20 steps.

B. Black-box model

Initially, the BB model was trained on the MIMO system. However, the velocity predictions diverged rapidly during training preventing the learning to converge. Therefore, the velocity and body rates were decoupled as two MIMO subsystems to be learned by two separate RNNs. The first RNN is trained to predict the body rates from the motor speeds. The second RNN uses the predicted body rates along with the motor speeds to predict the velocity. However, we train the second RNN on the *actual* body rates. This form of training resembles *teacher forcing* [27]. However, in an MS prediction scneario, the second RNN must use the *predicted* body rates.

C. Hybrid model

In contrast to the BB model, a hybrid model learns the full MIMO system. The model receives the motor speeds and generates prediction for the velocity and body rates *at the same time*. The drag coefficient parameters of the MM model is identified as part of the learning process. The identified values from the hybrid-serial model were not as consistent as the values form the hybrid-parallel model, implying the possibility that the MM module was not being effectively used. The identified parameters by the hybrid-parallel model were $k_t = 0.026 \pm 0.0132$ and $k_r = (2.1 \pm 1.6) \times 10^{-8}$.

D. Comparisons

In Figure 4, the WB performance is studied. In Figure 4a the SS prediction error distributions are plotted for the WB and the hybrid-parallel models and the performance boost of the hybrid model is shown. In Figure 4b, the WB is used in an MS prediction scenario for 20 steps. It is observed that the prediction error rapidly diverges. Therefore, the WB will not be further studied as it fails to reliably perform in an MS prediction scenario.

Figure 5 compares the prediction performance of the BB model, the hybrid-serial and the hybrid-parallel configurations. For each model, LSTM networks are used with and without TDLs. For the TDL, the buffer size is 10. Our experiments show that incorporating TDL on average slightly improves the BB and the hybrid-serial configurations at the cost of slight increase in the network size. However, for the parallel configuration the TDL causes slight decrease in the performance. Note that we have used the actual body rates for the BB velocity prediction. For an MS prediction,

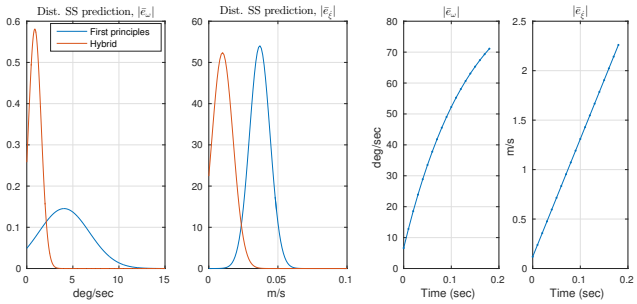

(a) SS prediction (b) 20 step prediction

Fig. 4: WB prediction performance

it means we have used the body rate measurements over the prediction horizon which contradicts the assumption in our defined MS prediction problem. Nevertheless, the hybrid model outperforms the BB model. Later we will use the predicted body rates to generate velocity prediction for the BB model.

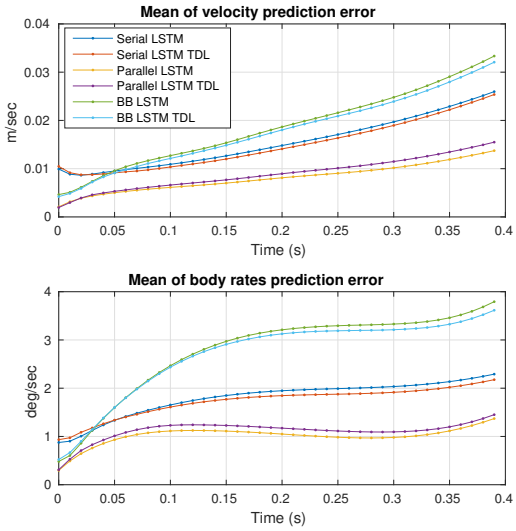

Fig. 5: Comparison between the BB and the hybrid models.

Our experiments show that the hybrid-parallel model outperforms the hybrid-serial architecture. The experiments were ran for four prediction lengths, $T = 50, 100, 150$ and 200 steps, which correspond to 0.5, 1.0, 1.5 and 2.0 seconds flight time, respectively. However, as the performance trends are similar, we study only 50 and 200 steps. Note that the first 10 steps are used for the initialization procedure, hence, the prediction lengths are $T - 10$.

In Figures 6, 7, 8 and 9 and we compare the error distributions of the BB model and the hybrid-parallel model throughout the MS prediction. For the BB model, we use the predicted body rates to predict velocity. For the shortest prediction length $(0.4s)$ the hybrid-parallel model improves the body rate error by 50% compared to the BB model and the velocity error by about $20\times$. The reason that the BB model performs poorly on the velocity prediction, as stated before, is that we use the predicted body rates.

For the longer prediction horizons, the BB predicted body rate initially performs worse, however, in the long run it performs better than the hybrid model. One reason for this behaviour is that the MM module in the hybrid model limits the exploration capacity of the OM module, where as in the full BB model such a bound does not exists. The LSTMs in the BB model are free to explore the entire weight space and they can accumulate relevant information over longer time to perform better. For the velocity, we see that BB still performs worse, however a slight decrease is seen on the later predictions which is similar to the behaviour in the body rate prediction.

In Figure 10 the error distributions of the MM output are illustrated before compensation for each prediction length. This results show the importance of RNN network initialization. This is due to the fact that the first prediction error from the MM is none-zero and hence the network has to immediately compensate for that. The improvement is shown by comparing with their respective compensated error (hybrid-model outputs).

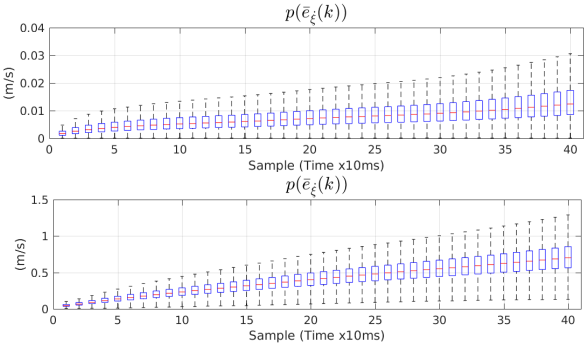

Fig. 6: Comparison of the velocity error distribution between the BB (top) and hybrid-parallel (bottom) model ($T = 50$).

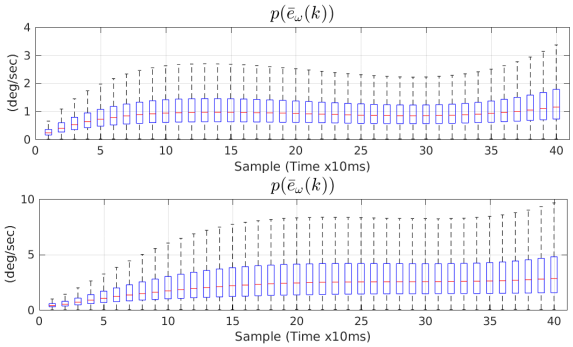

Fig. 7: Comparison of the body rate error distribution between the BB (top) and hybrid-parallel (bottom) model ($T = 50$)

VI. Conclusion

We have proposed a hybrid model for a real quadrotor in a Multi-Step prediction scenario. Our model takes advantage of prior knowledge imposed by the first principle model and in conjunction with deep RNNs, it learns the underlying quadrotor dynamics from a real quadrotor dataset. Our approach significantly outperforms existing models based on

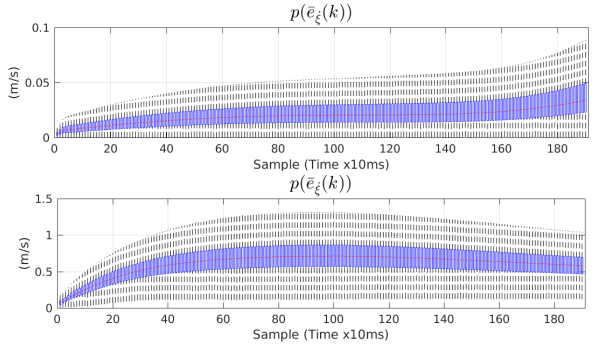

Fig. 8: Comparison of the velocity error distribution between the BB (top) and hybrid-parallel (bottom) model ($T = 200$).

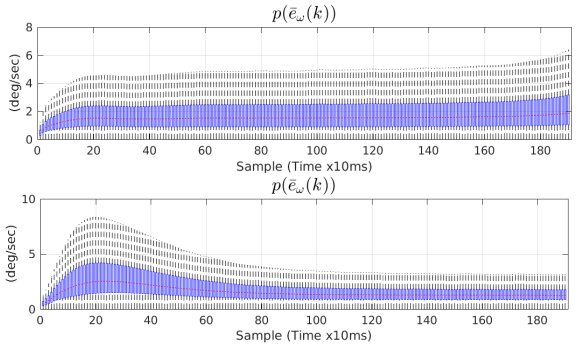

Fig. 9: Comparison of the body rate error distribution between the BB (top) and hybrid-parallel (bottom) model ($T = 200$).

first principle modelling as well as black box modelling. Our predictions show competitive performance with the state-of-the art quadrotor modelling techniques.

REFERENCES

[1] A. G. Parlos, O. T. Rais, and A. F. Atiya, "Multi-step-ahead prediction using dynamic recurrent neural networks," *Neural networks*, vol. 13, no. 7, pp. 765–786, 2000.

[2] R. Boné and M. Crucianu, "Multi-step-ahead prediction with neural networks: a review," *9emes rencontres internationales: Approches Connexionnistes en Sciences*, vol. 2, pp. 97–106, 2002.

[3] L. Ljung and T. Söderström, *System identification*. MIT Press, 1983.

[4] T. P. Bohlin, *Practical grey-box process identification: theory and applications*. Springer Science & Business Media, 2006.

[5] T. Madani and A. Benallegue, "Adaptive control via backstepping technique and neural networks of a quadrotor helicopter," in *Proceedings of the 17th World Congress of The Internaional Federation of Automatic Control*, 2008.

[6] D. Sonntag, "A study of quadrotor modelling," 2011.

[7] Q. Li, "Grey-box system identification of a quadrotor unmanned aerial vehicle," 2014.

[8] R. L. W. Choi, "Modelling and model based control design for rotorcraft unmanned aerial vehicle," 2014.

[9] M. Bäck, "Grey-box modelling of a quadrotor using closed-loop data," 2015.

[10] W. Wei, *Development of an Effective System Identification and Control Capability for Quad-copter UAVs*. University of Cincinnati, 2015.

[11] I. Kugelberg, "Black-box modeling and attitude control of a quad-copter," 2016.

[12] H. Voos, "Nonlinear control of a quadrotor micro-uav using feedback-linearization," in *Mechatronics, 2009. ICM 2009. IEEE International Conference on*. IEEE, 2009, pp. 1–6.

[13] G. M. Hoffmann, H. Huang, S. L. Waslander, and C. J. Tomlin, "Precision flight control for a multi-vehicle quadrotor helicopter testbed," *Control engineering practice*, vol. 19, no. 9, pp. 1023–1036, 2011.

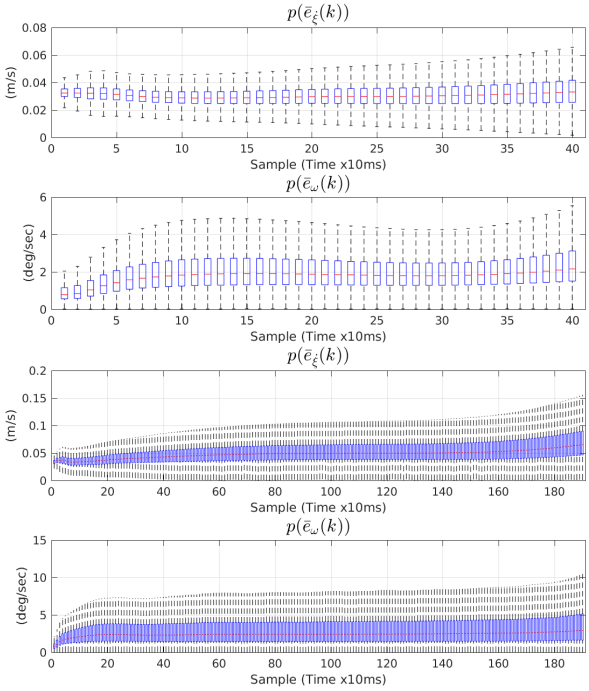

Fig. 10: Uncompensated output of the MM module for the velocity and body rate predictions.

[14] A. Freddi, A. Lanzon, and S. Longhi, "A feedback linearization approach to fault tolerance in quadrotor vehicles," in *Proceedings of The 2011 IFAC World Congress, Milan, Italy*, 2011.

[15] A. Punjani and P. Abbeel, "Deep learning helicopter dynamics models," in *Robotics and Automation (ICRA), 2015 IEEE International Conference on*. IEEE, 2015, pp. 3223–3230.

[16] S. Bansal, A. K. Akametalu, F. J. Jiang, F. Laine, and C. J. Tomlin, "Learning quadrotor dynamics using neural network for flight control," in *2016 IEEE 55th Conference on Decision and Control (CDC)*, Dec 2016, pp. 4653–4660.

[17] A. Vargas, M. Ireland, and D. Anderson, "System identification of multi-rotor uavs using echo state networks," 2015.

[18] N. Mohajerin and S. Waslander, "Modular deep recurrent neural network: Application to quadrotors," in *2014 IEEE International Conference on Systems, Man and Cybernetics*, 2014.

[19] ——, "Modelling a quadrotor vehicle using a modular deep recurrent neural network," in *2015 IEEE International Conference on Systems, Man and Cybernetics*, 2015.

[20] N. Mohajerin and S. L. Waslander, "State initialization for recurrent neural network modeling of time-series data," in *Neural Networks (IJCNN), 2017 International Joint Conference on*. IEEE, 2017, pp. 2330–2337.

[21] J. E. Sierra and M. Santos, "Modelling engineering systems using analytical and neural techniques: Hybridization," *Neurocomputing*, 2017.

[22] J. Schmidhuber and S. Hochreiter, "Long short-term memory," *Neural Computation*, vol. 9, no. 8, pp. 1735–1780, 1997.

[23] K. Greff, R. K. Srivastava, J. Koutník, B. R. Steunebrink, and J. Schmidhuber, "Lstm: A search space odyssey," *IEEE transactions on neural networks and learning systems*, 2017.

[24] H. Sak, A. Senior, and F. Beaufays, "Long short-term memory recurrent neural network architectures for large scale acoustic modeling," in *Fifteenth Annual Conference of the International Speech Communication Association*, 2014.

[25] S. Haykin, *Neural Networks: A Comprehensive Foundation*. Prentice-Hall, 1999.

[26] M. A. et al, "TensorFlow: Large-scale machine learning on heterogeneous systems," 2015, software available from tensorflow.org. [Online]. Available: http://tensorflow.org/

[27] K. Narendra and K. Parthasarathy, "Identification and control of

dynamical systems using neural networks," *IEEE Transactions on Neural Networks*, vol. 1, no. 1, pp. 4 –27, March 1990.